Neurobiology of Aging 94 (2020) 71–80

Contents lists available at ScienceDirect

Neurobiology of Aging

journal homepage: www.elsevier.com/locate/neuaging

Single-subject gray matter networks predict future cortical atrophy in preclinical Alzheimer's disease

Ellen Dicks [a,*], Wiesje M. van der Flier [a,b], Philip Scheltens [a], Frederik Barkhof [c,d], Betty M. Tijms [a], for the Alzheimer's Disease Neuroimaging Initiative [1]

[a] Department of Neurology, Alzheimer Center Amsterdam, Amsterdam Neuroscience, Vrije Universiteit Amsterdam, Amsterdam UMC, Amsterdam, the Netherlands
[b] Department of Epidemiology and Biostatistics, Amsterdam Neuroscience, Vrije Universiteit Amsterdam, Amsterdam UMC, Amsterdam, the Netherlands
[c] Department of Radiology and Nuclear Medicine, Amsterdam Neuroscience, Vrije Universiteit Amsterdam, Amsterdam UMC, Amsterdam, the Netherlands
[d] Centre for Medical Image Computing, Medical Physics and Biomedical Engineering, UCL, London, United Kingdom

ARTICLE INFO

Article history:
Received 22 August 2019
Received in revised form 8 May 2020
Accepted 10 May 2020
Available online 21 May 2020

Keywords::
Alzheimer's disease
Amyloid
Atrophy
Preclinical
Single-subject gray matter networks

ABSTRACT

The development of preventive strategies in early-stage Alzheimer's disease (AD) requires measures that can predict future brain atrophy. Gray matter network measures are related to amyloid burden in cognitively normal older individuals and predict clinical progression in preclinical AD. Here, we show that within individuals with preclinical AD, gray matter network measures predict hippocampal atrophy rates, whereas other AD biomarkers (total gray matter volume, cerebrospinal fluid total tau, and Mini-Mental State Examination) do not. Furthermore, in brain areas where amyloid is known to start aggregating (i.e. anterior cingulate and precuneus), disrupted network measures predict faster atrophy in other distant areas, mostly involving temporal regions, which are associated with AD. When repeating analyses in age-matched, cognitively unimpaired individuals without amyloid or tau pathology, we did not find any associations between network measures and hippocampal atrophy, suggesting that the associations are specific for preclinical AD. Our findings suggest that disrupted gray matter networks may indicate a treatment opportunity in preclinical AD individuals but before the onset of irreversible atrophy and cognitive impairment.

1. Introduction

Alzheimer's disease (AD) is a neurodegenerative disorder that is the most common cause of dementia (Lobo et al., 2000; Plassman et al., 2007). Among the earliest pathological changes in AD is aggregation of amyloid beta into plaques (Bateman et al., 2012; Jansen et al., 2015), starting in the anterior cingulate cortex and the precuneus (Palmqvist et al., 2017; Villain et al., 2012; Villeneuve et al., 2015). Once amyloid has aggregated, it may take up to 10 years before atrophy starts (Bateman et al., 2012), which most prominently affects more distant brain areas in the medial temporal lobes (Chetelat et al., 2012; Dickerson et al., 2009; Whitwell et al., 2007) and is more closely related to cognitive decline (van Rossum et al., 2012). How amyloid aggregation in one brain area eventually leads to neurodegeneration in more distant brain areas remains largely unclear. For development of preventive strategies, it is important to predict future brain atrophy, as this may aid in identifying which individuals with abnormal amyloid but still normal cognition (i.e. preclinical AD; Sperling et al., 2011) will show disease progression but before the onset of irreversible atrophy.

Amyloid aggregation disrupts local synaptic functioning (Koffie et al., 2009; Shankar et al., 2008; Walsh et al., 2002), potentially leading to disruptions of large-scale brain connectivity networks (Buckner et al., 2005; Kuchibhotla et al., 2008; Kurudenkandy et al.,

* Corresponding author at: Alzheimer Center and Department of Neurology, Amsterdam UMC, Location VUmc PO Box 7057, 1007 MB, Amsterdam, the Netherlands. Tel.: +31 204440183; fax: +31 204440183.
E-mail addresses: e.dicks@amsterdamumc.nl, ellendicks.ac@gmail.com (E. Dicks).

[1] Data used in preparation of this article were obtained from the Alzheimer's Disease Neuroimaging Initiative (ADNI) database (adni.loni.usc.edu). As such, the investigators within the ADNI contributed to the design and implementation of ADNI and/or provided data but did not participate in analysis or writing of this report. A complete listing of ADNI investigators can be found at: http://adni.loni.usc.edu/wp-content/uploads/how_to_apply/ADNI_Acknowledgement_List.pdf.

0197-4580/
https://doi.org/10.1016/j.neurobiolaging.2020.05.008

2014; Palmqvist et al., 2017; Palop et al., 2007; Sperling et al., 2009). One approach to measure brain networks is based on intracortical similarity on structural magnetic resonance imaging (MRI) (i.e. gray matter connectivity; Mechelli et al., 2005; Tijms et al., 2012). Intracortical similarity has been associated with coordinated growth patterns (Alexander-Bloch et al., 2013b), functional coactivation (Alexander-Bloch et al., 2013a) and axonal connectivity (Gong et al., 2012). We and others have shown that gray matter networks are disrupted in AD (He et al., 2008; Pereira et al., 2016; Tijms et al., 2013a,b; Yao et al., 2010), associated with cognitive impairment (Tijms et al., 2013a, 2014), and related to faster disease progression and cognitive decline in the predementia stage of AD (Dicks et al., 2018; Tijms et al., 2018; Verfaillie et al., 2018). Furthermore, disrupted gray matter network organization has been associated with aggregating amyloid in cognitively normal individuals (ten Kate et al., 2018; Tijms et al., 2016) and before overt atrophy is evident (Voevodskaya et al., 2018). Taken together, these findings suggest that gray matter network measures might have use to identify those individuals who will progress to AD dementia in the earliest, preclinical stages of AD *and before* the onset of irreversible atrophy. In a cross-sectional study, Seeley et al. previously showed that atrophy patterns in patients with AD dementia reflect brain regions that show both strong functional coactivation as well as covariation in gray matter volume across a group of cognitively normal individuals, suggesting that regions that are highly interconnected share vulnerability for neurodegeneration (Seeley et al., 2009). It could be hypothesized that gray matter network disruptions due to amyloid aggregation in one region of the brain may capture the earliest neurodegenerative changes in preclinical AD and predict future atrophy in more distant regions. However, as previous findings were based on cross-sectional studies and/or used only 1 network per group of individuals, it is still unclear whether gray matter network disruptions can predict the rate and location of future atrophy *within* individuals.

In this study, we used a subject-specific approach to construct gray matter networks in individuals with preclinical AD and investigated whether altered gray matter network measures at baseline could predict the rate and location of future atrophy. We first compared the predictive performance for future hippocampal atrophy between whole-brain gray matter network measures and other AD markers that have been previously associated with reduced gray matter volume (i.e. total gray matter volume, cerebrospinal fluid [CSF] total tau levels, and Mini-Mental State Examination [MMSE] scores). We then investigated whether gray matter network measures specifically in regions, where amyloid has previously been shown to start aggregating (i.e. anterior cingulate and precuneus; Palmqvist et al., 2017; Villeneuve et al., 2015), could predict the rate of subsequent atrophy in other brain areas within single individuals with preclinical AD. We also performed analyses in cognitively unimpaired, age-matched individuals without evidence of amyloid or tau pathology to study whether results were specific for preclinical AD, and additionally investigated the effects of clinical progression, tau pathology, and sex on network disruptions and their associations with future hippocampal atrophy.

2. Methods

2.1. Participants

Data used in the preparation of this article were obtained from the Alzheimer's Disease Neuroimaging Initiative (ADNI) database (http://adni.loni.usc.edu). The ADNI was launched in 2003 as a public-private partnership, led by the principal investigator Michael W. Weiner, MD. The primary goal of ADNI has been to test whether serial MRI, positron emission tomography (PET), other biological markers, and clinical and neuropsychological assessment can be combined to measure the progression of mild cognitive impairment and early AD. ADNI was approved by the institutional review board of all participating institutions, and written informed consent was obtained from all participants at each site.

We selected all participants with preclinical AD from ADNI as defined by normal cognition and abnormal amyloid CSF markers at baseline who had at least 1 year of MRI follow-up with a minimum of 2 structural MRI scans available. In addition, we included cognitively unimpaired, age-matched individuals without amyloid or tau pathology as a control group (control; $n = 71$), to determine whether results were specific for individuals with preclinical AD. Details of clinical diagnostic criteria have been previously described (Aisen et al., 2015; Petersen et al., 2010). Briefly, cognitively normal individuals had to have a clinical dementia rating (CDR) score of 0, an MMSE score between 24 and 30, and no impaired memory as based on education-adjusted cutoffs on the delayed recall subtest of the Logical Memory II subscale of the Wechsler Memory Scale—Revised (Aisen et al., 2015; Petersen et al., 2010). In total, 110 preclinical AD individuals were included with a median of 5 (min-max: 2-10) repeated MRI scans over a median follow-up time of 2.2 (min-max: 1-9) years, during which time 25% of individuals progressed to mild cognitive impairment or dementia because of AD. Diagnoses of mild cognitive impairment or dementia were based on cognitive impairment on the CDR, MMSE, or logical memory—delayed recall (for cutoff scores, refer to the studies by Aisen et al., 2015; Petersen et al., 2010). In addition, patients with dementia had to have a clinical diagnosis of probable AD as per the NINCDS-ADRDA criteria (McKhann et al., 1984).

We used CSF measures for amyloid beta 1-42 to determine amyloid abnormality and additionally CSF total tau to determine tau abnormality in control individuals. Amyloid beta 1-42 and total tau were measured with the multiplex xMAP Luminex platform (Luminex Corp, Austin, TX, USA) and INNO-BIA AlzBio3 (Innogenetics, Ghent, Belgium) immunoassay kit-based reagents (Shaw et al., 2009). Abnormal amyloid was indicated by levels <192 pg/mL, and abnormal tau was indicated by levels of >95 pg/mL (Shaw et al., 2009).

2.2. MRI acquisition & preprocessing

Image acquisition details and initial preprocessing have been previously described (http://adni.loni.usc.edu/methods/mri-analysis/; Jack et al., 2008). We downloaded all 3-dimensional T1-weighted structural scans that were preprocessed with gradient nonlinearity correction, B1 inhomogeneity, and/or N3 correction and of sufficient quality from the ADNI LONI Image & Data Archive (date of last access: 29.03.2017; $n = 534$). Scans that were acquired using different field strengths within subjects were excluded.

First, all images were reoriented with FSL (v5.0.6). Next, to reduce bias in longitudinal registration (Reuter et al., 2012), we created a subject-specific median template image with FreeSurfer (v5.3.0) to which all longitudinal scans were co-registered. We then segmented images into gray matter, white matter, and CSF with the Markov random fields parameter set to 2 and default settings for all other parameters. Co-registration and segmentation was performed with SPM12 running under Matlab (v.7.12.0.635). Finally, using the subject-specific inversed normalization parameters, the automated anatomical labeling atlas (AAL) (Tzourio-Mazoyer et al., 2002) was warped from standard space to subject space, and we calculated regional gray matter volumes for each of the 90 cortical and subcortical AAL areas. Total intracranial volume was computed as the sum of gray matter, white matter, and CSF volumes in cm^3, and gray matter volume was normalized to baseline total

intracranial volume. All gray matter segmentations and subject-specific atlases were visually checked for quality.

2.3. Single-subject gray matter network measures

Single-subject gray matter networks were reconstructed from subject space gray matter segmentations of baseline MRI scans using an automated method (https://github.com/bettytijms/Single_Subject_Grey_Matter_Networks), which has been described previously (Tijms et al., 2012). Briefly, nodes were defined as small regions of interest of 3 × 3 × 3 voxel cubes and connected when they showed similar gray matter structure as defined by a significant correlation between voxels of 2 nodes. By defining nodes as cubes, both spatial information (i.e. the folding structure of the cortex) and local gray matter values were used to assess the correlation between nodes. Because the cortex is a curved object, regions of interest could be located at an angle to each other, thus possibly decreasing correlations. Therefore, for each pairwise comparison, the seed cube was rotated by an angle with multiples of 45° to identify the maximum correlation coefficient. Next, we binarized the networks using subject-specific thresholds based on empirical null model distributions (Noble, 2009) that ensured that all individuals showed a similar chance of 5% false-positive connections within the network. A detailed description of the single-subject network extraction technique can be found in the study Tijms et al., 2012. For each single-subject gray matter network, we computed the network size, degree, connectivity density, clustering coefficient, and path length. The network size is the number of nodes (i.e. cubes) in the network. The degree corresponds to the number of connections per node. The connectivity density is the ratio of present connections divided by the number of possible connections in the network. The clustering coefficient indicates the interconnectedness of neighboring nodes and the path length corresponds to the average shortest paths between all nodes in the network (Rubinov and Sporns, 2010). To obtain network measures for the precuneus and anterior cingulate, we averaged measures across nodes that were labeled in accordance with the AAL atlas. Global network measures were obtained by averaging measures across all nodes of the network. We additionally computed the global normalized clustering coefficient, normalized path length (gamma, lambda), and small-world coefficient for the whole brain to estimate how these network measures deviated from randomly organized networks as follows: Gamma and lambda were computed by normalizing clustering coefficient and path length values with the respective mean values of 5 randomized reference networks, which kept the degree distribution intact (Maslov and Sneppen, 2002). The small-world coefficient is defined as the ratio of gamma to lambda (Humphries and Gurney, 2008). All network measures were calculated using functions from the Brain Connectivity Toolbox (https://sites.google.com/site/bctnet/; Rubinov and Sporns, 2010) adjusted for large-sized networks.

2.4. Statistical analysis

Cortical atrophy was determined by fitting linear mixed models for each AAL area with longitudinal gray matter volume as outcome and time from baseline as predictor. We fitted random slopes for time and intercepts for individuals and assumed an unstructured covariance structure using the R package "lme4" (Bates et al., 2015). We first assessed whether global network measures could predict future hippocampal atrophy, as a prominent region for AD-associated atrophy. Repeated hippocampal volume over time was used as the outcome (i.e. hippocampal volume at baseline, hippocampal volume at visit 1, hippocampal volume at visit 2, and so on) and baseline network measures (NM), time, and their interaction as the predictors.

$$Hippocampal\ volume = \beta_{Intercept} + \beta_{NM}NM + \beta_{Time}Time + \beta_{NM\times Time}NM \times Time + (1 + Time|Subject)$$

We repeated these analyses including clinical progression as a main term and interaction effect (i.e. network measure × time × clinical progression) to investigate whether the observed effects were stronger for those individuals who progressed during follow-up. Similarly, we also investigated the effects of tau and sex on baseline network disruptions and associations with future hippocampal atrophy by including tau abnormality or sex as additional interaction term in the analyses. We qualitatively compared the predictive performance between global network measures and other markers that are associated with reduced gray matter volume (i.e. CSF total tau, MMSE scores, and total gray matter volume). For visualization purposes and to aid in comparison of the predictive performances, we additionally performed linear regression analyses with subject-specific hippocampal atrophy slopes as outcome and baseline whole-brain gray matter network measures or AD markers as predictor.

$$\Delta\ Hippocampal\ volume = \beta_{Intercept} + \beta_{NM}NM$$

To investigate whether altered network measures in early amyloid accumulating regions (i.e. anterior cingulate and precuneus) could predict the rate and location of future atrophy, we repeated analyses as for hippocampal volume but with longitudinal local gray matter volumes for each AAL region as the outcome and local network measures of the anterior cingulate or precuneus, time and their interaction as the predictors. All local gray matter volumes and network measures were standardized across regions as per the mean baseline values of individuals who remained cognitively stable to aid interpretation of the results. We also performed analyses for hippocampal and whole-brain atrophy in control individuals, who were age-matched to the original sample using the R package "Matching" (Sekhon, 2008) to study specificity of results for preclinical AD. All analyses were adjusted for age, gender, field strength, and total gray matter volume. Statistical analyses were performed in R (version 3.4.4, 2018-03–15) and Surf Ice (version 2017-08-08) was used to visualize regional results.

3. Results

3.1. Characteristics of the study sample

In this study, we selected all individuals from the ADNI cohort who had normal cognition and abnormal CSF levels of amyloid beta 1-42 at baseline and at least 1 year of MRI follow-up available (n = 110). Table 1 shows the baseline characteristics of the included sample and by clinical progression. Individuals were on average 75 ± 6 years of age, and 57 % were women. During follow-up (median [interquartile range] 2.2 [2–4] years), 28 participants (25%) showed clinical progression (n = 21 to prodromal AD and n = 7 to AD dementia). Progressing participants were on average older, had more MRI scans over a longer follow-up period available, and had higher total intracranial volume ($p < 0.05$). In addition, progressing participants had higher network size and degree (due to higher gray matter volume; $p < 0.065$) and lower gamma and small-world coefficient values at baseline ($p < 0.05$) and showed a tendency for lower lambda values than those who remained stable ($p < 0.065$). Over time, the total sample showed cortical atrophy with fastest rates observed in the hippocampus (β ± SE; left hippocampus: −0.15 ± 0.01, right hippocampus: −0.14 ± 0.01; all p

Table 1
Baseline characteristics of the total sample and by clinical progression

Characteristic	Total	Stable	Progression
N	110	82 (75%)	28 (25%)
Female	63 (57%)	51 (62%)	12 (43%)
Age (y)	74.871 (6.084)	74.05 (6.357)	77.275 (4.487)[c]
MMSE	29 (29–30)	29 (29–30)	29 (28–30)
Education (y)	16 (14–18)	16 (14–18)	16 (14–18)
CSF Aβ 1-42 in pg/mL	149.166 (25.393)	150.138 (25.626)	146.321 (24.934)
CSF total tau in pg/mL	73.845 (38.418)	71.063 (39.216)	81.989 (35.391)
Abnormal total tau >93 pg/mL	30 (27%)	20 (24%)	10 (36%)
Total intracranial volume in cm^3	1439.591 (144.808)	1417.037 (145.665)	1505.643 (122.185)[d]
Gray matter volume in cm^3	0.601 (0.067)	0.597 (0.069)	0.614 (0.064)
[a]Normalized gray matter volume in cm^3	0.419 (0.04)	0.423 (0.038)	0.409 (0.043)
Number of repeated MRI	5 (4–6)	5 (4–5.8)	6 (3.8–7.2)[c]
Follow-up time (y)	2.2 (2–4)	2.1 (2–4)	4 (2.2–6)[d]
Size	6753.082 (606.983)	6658.341 (616.29)	7030.536 (490.741)[d]
Degree	1204.765 (132.373)	1191.003 (129.279)	1245.069 (135.429)[b]
Connectivity density	17.845 (1.14)	17.896 (1.092)	17.697 (1.279)
Clustering	0.49 (0.022)	0.491 (0.021)	0.485 (0.023)
Path length	1.998 (0.021)	2 (0.021)	1.993 (0.022)
Gamma	1.688 (0.079)	1.698 (0.076)	1.661 (0.084)[c]
Lambda	1.097 (0.012)	1.098 (0.012)	1.093 (0.012)[b]
Small-world coefficient	1.539 (0.058)	1.545 (0.055)	1.519 (0.064)[c]

CSF, cerebrospinal fluid; MRI, magnetic resonance imaging.
Data are presented as N (%), mean (SD) or median (IQR) where appropriate.
[a] Grey matter volume was normalized to total intracranial volume.
[b] $p < 0.065$.
[c] $p < 0.05$.
[d] $p < 0.01$.

< 0.001) (Figs. 1 and 2A). Individuals who progressed during follow-up showed faster hippocampal atrophy rates than those who remained stable ($p_{interaction}$ < 0.001; Fig.2A; see also Supplementary Fig. 1 and Supplementary Table 1). Additional analyses performed in a subset of individuals who had amyloid PET available showed highest uptake in the precuneus as compared with controls with normal CSF amyloid levels (see Supplementary Fig. 2).

3.2. Prediction of hippocampal atrophy rates

We first investigated whether baseline global network measures and other AD markers that have been related to cognitive decline (MMSE scores, CSF total tau, and total gray matter volume) could predict hippocampal atrophy rates. Baseline MMSE scores, CSF total tau, and whole-brain gray matter volume did not show associations with subject-specific hippocampal atrophy rates (all $p > 0.05$; Table 2) (see also Fig. 2B–D). Lower connectivity density and lower clustering at baseline predicted faster subsequent hippocampal atrophy (β ± SE; both 0.04 ± 0.01; $p < 0.005$; Table 2) (see also Fig. 2E–F). Analyses including disease progression as an additional interaction term did not show significant interaction effects (all $p >$ 0.05; see Supplementary Table 1), suggesting that the association of baseline network measures and subsequent atrophy was similar for individuals who remained stable and those who showed clinical progression during follow-up.

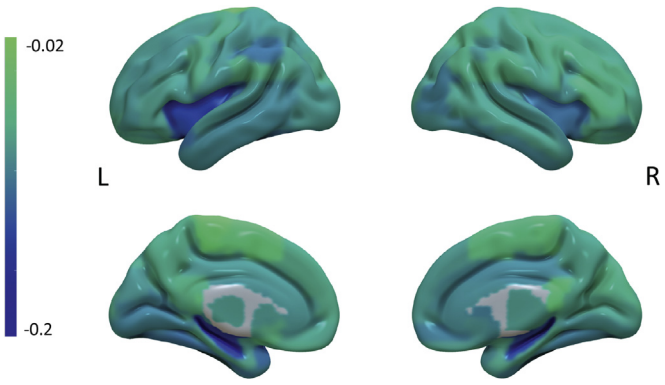

Fig. 1. Surface plots of regional atrophy rates over time. The color bar indicates standardized betas of regional atrophy rates and was obtained with linear mixed models. Analyses were adjusted for age, sex, education, field strength, and total intracranial volume. Subcortical structures are plotted in ventricular areas as approximation. Abbreviations: L, left hemisphere; R, right hemisphere. (For interpretation of the references to color in this figure legend, the reader is referred to the Web version of this article.)

3.3. Prediction of whole-brain atrophy patterns

We further investigated whether network measures in the anterior cingulate and precuneus could predict the spatiotemporal pattern of atrophy. Both local clustering and path length values showed associations with subsequent gray matter atrophy, for specific parts of the brain (Fig. 3, see Supplementary Fig. 3 for cross-sectional relationships): Lower clustering values in the anterior cingulate and precuneus of both hemispheres were associated with faster atrophy in mostly temporal regions, including the right superior, middle temporal pole, hippocampus, and left parahippocampal gyrus (all $p < 0.05$; Fig. 3A–D). Higher path length values in the right anterior cingulate and bilateral precuneus were associated with faster atrophy in mostly frontal regions, including the right superior, middle frontal gyrus, and left middle cingulate (all $p < 0.05$; Fig. 3E–H). Gray matter volumes of the anterior cingulate or precuneus did not predict future hippocampal atrophy rates (all $p > 0.05$; see Supplementary Table 2), indicating that network measures contain information that relate to the rate of hippocampal atrophy beyond volumetric measures.

3.4. Prediction of atrophy rates in control individuals

We then performed analyses in cognitively unimpaired, amyloid/tau normal, age-matched individuals (control) to investigate

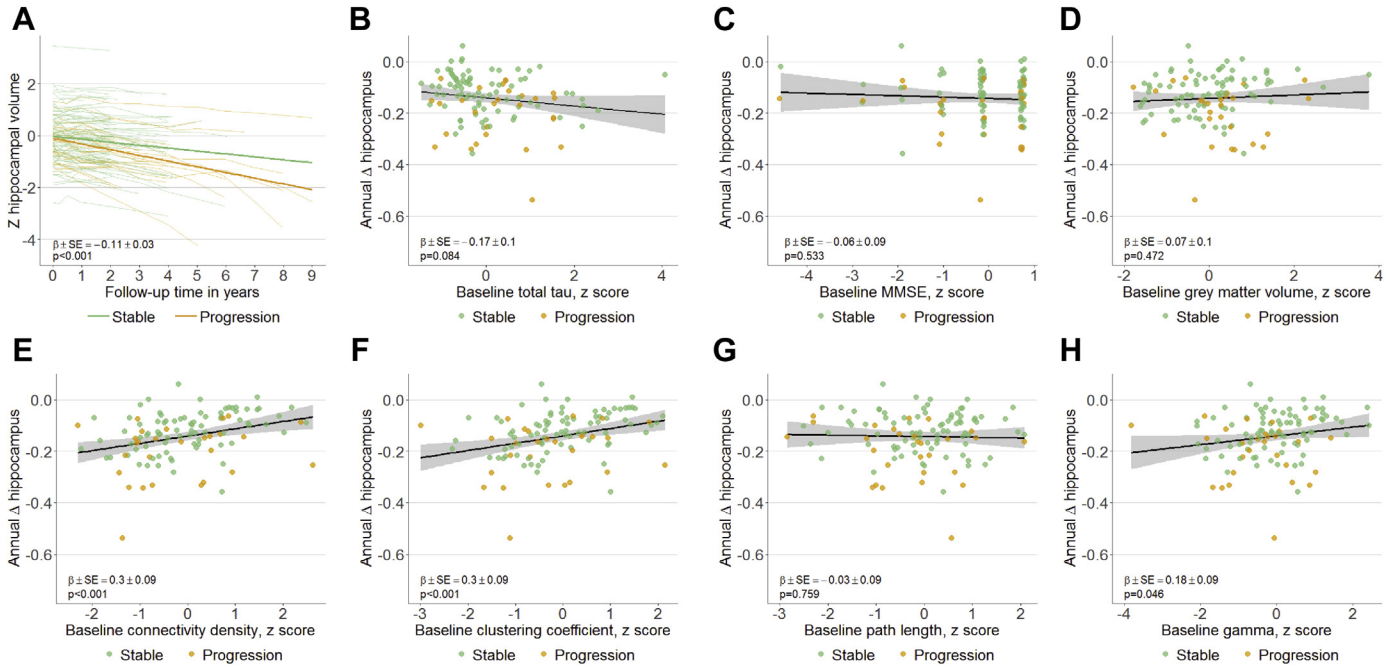

Fig. 2. Association of baseline AD markers and whole-brain gray matter network measures with hippocampal atrophy rates. Predicted decline in hippocampal volume over time (A) and associations of baseline AD markers (B)–(D) and whole-brain gray matter network measures (E)–(H) with subject-specific annual hippocampal atrophy rates. Longitudinal decline in hippocampal volume over time was estimated with linear mixed models adjusted for age, sex, field strength, and total gray matter volume. To aid in comparison of predictive performances we report standardized β ± SE for (B)–(H) as estimated with linear regression analyses. Linear regression analyses included the terms for subject-specific annual hippocampal atrophy rates as outcome and baseline values of AD markers (B)–(D) or gray matter network measures (E)–(H) as the respective predictor. Note that standardized betas for (B)–(H) estimated with linear regression analyses do not correspond to the betas in Table 2, which were estimated with linear mixed models.

whether the observed effects were specific for preclinical AD individuals. At baseline, controls had more years of education ($p < 0.05$) and slightly higher gray matter volume ($p < 0.065$) than preclinical AD (see Supplementary Table 3). We observed slightly higher path length values ($p < 0.065$) and higher gamma, lambda, and small-world coefficient values (all $p < 0.05$) for control than those for preclinical AD, suggesting that networks were more random in preclinical AD individuals. Over time, controls also showed cortical atrophy with the steepest rate in the left hippocampus (β ± SE; −0.1 ± 0.01; $p < 0.001$; see Supplementary Fig. 4), albeit at a much slower rate than preclinical AD. We found no effects of baseline whole-brain gray matter network measures or other AD markers (i.e. CSF total tau, MMSE, and total gray matter volume) on the rate of future hippocampal atrophy in control individuals (see Supplementary Table 4). On a regional level, higher baseline clustering and path length values of the anterior cingulate and precuneus were associated with faster atrophy rates in mostly frontal and temporal regions but not the hippocampus (see Supplementary Fig. 5; see Supplementary Fig. 6 for cross-sectional relationships).

Table 2
Effects of baseline AD markers and gray matter network measures on cross-sectional and longitudinal hippocampal volume

Predictor	Cross-sectional effects	Longitudinal effects
MMSE	0.11 ± 0.07	−0.01 ± 0.01
CSF total tau	0 ± 0.08	−0.02 ± 0.01
Gray matter volume	0.63 ± 0.07[b]	0 ± 0.01
Gray matter network measures		
Size	0.04 ± 0.1	−0.02 ± 0.01
Degree	−0.11 ± 0.1	0.01 ± 0.01
Connectivity density	−0.06 ± 0.06	0.04 ± 0.01[a]
Clustering	−0.04 ± 0.07	0.04 ± 0.01[a]
Path length	0.1 ± 0.05	−0.01 ± 0.01
Gamma	0.07 ± 0.07	0.02 ± 0.01
Lambda	0.09 ± 0.06	0.02 ± 0.01
Sigma	0.06 ± 0.08	0.02 ± 0.01

AD, Alzheimer's disease; CSF, cerebrospinal fluid.
Data are presented as β ± SE. Linear mixed models included the terms for the baseline values of the respective predictor (e.g., baseline MMSE), follow-up time in years and their interaction (e.g., baseline MMSE × time). Cross-sectional effects represent the association between AD markers or gray matter network measures and hippocampal volume when time is held constant and are given by the main term for the respective predictor. Longitudinal effects describe the association between baseline AD markers or gray matter network measures on the rate of change in hippocampal volume over time and are given by the interaction term for the respective AD marker or network measure × time. All analyses were corrected for age and gender, and additionally adjusted for field strength for gray matter volume, and field strength and baseline gray matter volume for gray matter network measures.
[a] $p < 0.01$.
[b] $p < 0.001$. p-values are adjusted with the false discovery rate.

3.5. *Effect of tau and sex on network disruptions and associations with hippocampal atrophy rates*

Finally, we investigated the potential influences of tau abnormality and sex on our analyses. Individuals with abnormal levels of total tau (n = 30) were on average older, had lower levels of CSF amyloid beta 1-42, and had lower connectivity density and clustering values at baseline than those with normal levels of tau (n = 80) ($p < 0.05$; see Supplementary Table 5). There was no effect of tau abnormality on hippocampal atrophy rates over time (see Supplementary Table 6). When including tau abnormality as additional interaction term with the predictors for hippocampal atrophy we observed no significant effects, suggesting that individuals with abnormal and normal tau levels show similar associations between AD markers or gray matter network measures and hippocampal atrophy rates (all $p_{interaction} > 0.05$; Supplementary Table 6).

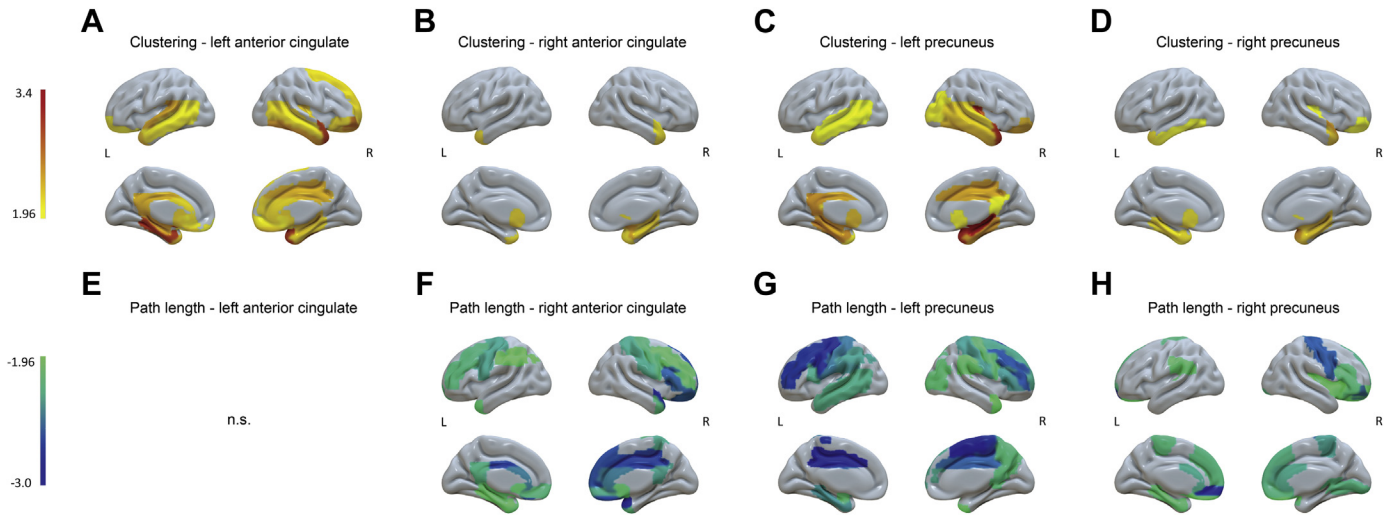

Fig. 3. Longitudinal effects of baseline precuneal and anterior cingulate network measures on regional atrophy over time. The color bar indicates the effect strength as t ratios, which were obtained with linear mixed model analyses with longitudinal regional gray matter volume as outcome and time, baseline network measure (e.g., clustering in the left anterior cingulate for panel a) and their interaction (time × network measure) as predictors. Analyses were adjusted for age, sex, field strength, and total gray matter volume. Subcortical structures are plotted in ventricular areas as approximation. Abbreviations: L, left hemisphere; R, right hemisphere; n.s., not significant. (For interpretation of the references to color in this figure legend, the reader is referred to the Web version of this article.)

Comparing female with male individuals with preclinical AD, male individuals were on average older, higher educated, and had higher total intracranial volume and gray matter volume, whereas they showed lower normalized gray matter volume than female preclinical AD individuals ($p < 0.05$; Supplementary Table 7). Male individuals further showed higher network size and degree and lower lambda values at baseline. Both sexes had similar hippocampal atrophy rates over time ($p_{interaction} > 0.05$; Supplementary Table 8). Repeating analyses for hippocampal atrophy including sex as an additional interaction term showed stronger associations between connectivity density and clustering values with future hippocampal atrophy rates in female preclinical AD individuals than in male individuals (interaction $\beta \pm SE$; both -0.05 ± 0.02, $p < 0.05$; Supplementary Table 8).

4. Discussion

The main result of our study is that individuals with preclinical AD who had low clustering and high path length values in early amyloid accumulating regions (i.e. anterior cingulate and precuneus) showed faster rates of subsequent atrophy in distant temporal and frontal regions. These results suggest that gray matter network measures may have use for identifying those individuals with preclinical AD who will show disease progression but before overt atrophy.

Individuals with preclinical AD are at increased risk for cognitive decline (Donohue et al., 2017; Parnetti et al., 2019; Vos et al., 2013). In our sample, 25% of individuals with preclinical AD progressed to mild cognitive impairment or dementia during follow-up, which is in line with previous estimates (Donohue et al., 2017; Parnetti et al., 2019; Vos et al., 2013). Furthermore, we observed that individuals with preclinical AD who later showed clinical progression had lower gamma values at baseline than those who remained stable, replicating our previous observations in another clinical cohort (Tijms et al., 2018). We further found that lower gray matter network measures at baseline predicted future hippocampal atrophy rates, whereas MMSE scores, CSF total tau, or total gray matter volume were not associated with individual rates of hippocampal atrophy, suggesting that network measures might capture more subtle neurodegenerative changes in very early preclinical stages. We did not find associations between network measures and future hippocampal atrophy rates in cognitively unimpaired age-matched individuals without amyloid or tau pathology, suggesting that these effects were specific for individuals with preclinical AD. A practical implication of our findings is that disrupted gray matter network measures may have use to identify those individuals with preclinical AD who will show disease progression but *before* the onset of irreversible atrophy and cognitive impairment. These results warrant further study in multiple independent data sets to investigate to what extent single-subject gray matter network measures can be used for e.g. patient identification in clinical trials.

One unresolved question in AD is the seeming spatiotemporal disconnect between the brain areas that are prone to aggregate amyloid early in the disease and medial temporal lobe atrophy in later disease stages. One hypothesis is that this might be driven by network (dis)connections: disruption of local synaptic functioning or connectivity due to amyloid (Koffie et al., 2009; Shankar et al., 2008; Walsh et al., 2002) and subsequent early neuronal cell death might lead to the loss of neurotrophic factors and/or absence of stimulation and thus atrophy of connected, but still more distant regions (Salehi et al., 2006; Seeley et al., 2009). A previous study showed that group-based structural covariance networks were indeed predictive for the locations of dementia type–specific atrophy patterns (Seeley et al., 2009). Our results further extent on that work by showing with our single-subject approach in preclinical AD that gray matter network measures in early amyloid accumulating regions can predict the rate of future atrophy and the anatomical location in *individual* persons. It should be noted, however, that gray matter networks reflect similarity in gray matter morphology, or atrophy patterns, which could exist in the absence of direct anatomical connections. Future studies should further investigate the neurobiological basis of these findings in combination with functional measures, such as functional MRI, or anatomical measures such as diffusion tensor imaging to further investigate in what way these distant regions are connected.

We also found that clustering coefficient and path length values were both related to subsequent atrophy in other distant and different regions of the brain, respectively in temporal and more frontal regions. This suggests that clustering and path length may reflect different aspects of neuronal degeneration as captured with

gray matter covariance networks. Clustering values indicate the interconnectedness of neighboring nodes, whereas path length measures the average shortest connections between all nodes in the entire network (Rubinov and Sporns, 2010). Possibly, lower clustering values (i.e. higher dissimilarity between neighboring nodes) reflect asynchronous atrophy of brain areas that were initially more similar to each other, whereas higher path length values (i.e. higher dissimilarity network-wide) potentially reflect asynchronous atrophy over the entire brain. Higher path length values were associated with faster future atrophy rates in predominantly frontal but still widespread areas of the brain. These regions are affected relatively late in the disease by tau pathology (Braak and Braak, 1991). It would be of interest for future studies to investigate how network alterations are associated with tau PET patterns. Our analyses in age-matched individuals without amyloid or tau pathology showed that higher clustering and path length values were most consistently associated with faster atrophy rates in frontal and temporal regions, which are more associated with "normal" aging processes (Fjell et al., 2009, 2014). Our finding that *higher* clustering values were associated with faster atrophy rates in these individuals suggests that neighboring regions show uniform neurodegenerative changes, presumably because of causes other than amyloid aggregation. Taken together, our findings suggest that lower clustering values might indicate AD specific atrophy, whereas higher path length values may indicate brain alterations that might reflect "normal" aging.

Our finding that preclinical AD showed globally lower path length values than controls but similar local associations of higher path length values with faster atrophy rates seems conflicting. Additional post hoc comparisons for local path length values showed that for preclinical AD, path length values were lower in mostly temporal regions than those of controls (Supplementary Fig. 7), which explains the differences in global path length values. Importantly, local path length values did not differ between the groups for our a priori defined target regions (i.e. anterior cingulate and precuneus). These results and our findings of similar local associations of higher path length values with faster atrophy rates further support that local path length values of the anterior cingulate and precuneus may reflect normal aging processes.

We found no associations between baseline MMSE scores, CSF total tau, or total gray matter volume with future hippocampal atrophy. Individuals with preclinical AD are still cognitively normal, and all had very high MMSE scores; so, the limited variability may explain the lack of predictive power for hippocampal atrophy. Furthermore, while changes in CSF total tau levels might occur relatively early in the disease process around the same time as atrophy in the hippocampus starts (Bateman et al., 2012), previous studies in individuals with preclinical AD also did not find direct associations between levels of CSF total tau and hippocampal (Wang et al., 2015) or entorhinal cortex atrophy (Desikan et al., 2011), which is in line with our findings. In addition, the observed associations between network measures and hippocampal atrophy did not depend on tau abnormality, and there were no differences between individuals with abnormal and normal levels of total tau in gray matter network disruptions (when accounting for age differences). Possibly, this indicates that CSF total tau levels and gray matter network disruptions may reflect different aspects of neurodegeneration. In line with this explanation, we previously also found that when predicting clinical progression in predementia AD, gray matter network measures contained predictive information in addition to CSF total tau levels (Tijms et al., 2018). Another previous study reported higher clustering values for individuals with abnormal levels of phosphorylated tau in CSF (Cantero et al., 2018). Possibly, the discrepancy with our results is that those individuals had normal amyloid levels, which has also been called "suspected non-AD pathophysiology" or "SNAP" (Jack et al., 2016) which reflects other disease causes than AD. Possibly, gray matter networks change differently depending on the underlying pathology, and future research should further investigate gray matter network alterations in SNAP populations. In addition, baseline total gray matter volume and precuneus and anterior cingulate volumes were not associated with future hippocampal atrophy, suggesting measurable, gross atrophy had not manifested yet in these individuals. These findings are in line with the notion that whole-brain gray matter network measures contain more information than more simple volumetric measures and suggest that network measures can predict hippocampal atrophy before irreversible overt atrophy and cognitive impairment manifest.

Finally, we observed that the associations of connectivity density and clustering values on hippocampal atrophy were stronger for female than for male individuals, whereas there were no significant differences between female and male individuals in baseline network measures or hippocampal atrophy rates over time. While to date, no study has investigated the effect of sex specifically on gray matter disruptions in AD, this result seems to be in line with other studies showing that female individuals who have higher levels of amyloid show relatively faster hippocampal atrophy or cognitive decline as compared with male individuals and as such hint at potentially higher susceptibility for AD pathology in women (Buckley et al., 2018; Koran et al., 2017). Future studies should further investigate potential implications of sex differences for individual patient-based measures on their e.g. gray matter network measure profile.

A potential limitation of our study is that although this is the largest longitudinal data set on preclinical AD available, with individuals followed up to nine years, the median follow-up duration was of 2.2 years. Therefore, we cannot exclude the possibility that more individuals would have shown disease progression if they would have been followed up for a longer period of time. Still, even within this relatively short median follow-up duration, we were able to observe a relationship between baseline gray matter network measures and subsequent atrophy. Another potential limitation of this study is that, while we ensured that scans of the same field strength were included within subjects, field strengths differed between individuals. To account for this, we included field strength as covariate in our analyses, and although we cannot exclude that this might have influenced our results, previous studies in ADNI have shown similar atrophy rate estimates for 1.5 Tesla and 3 Tesla scans (Dicks et al., 2019; Ho et al., 2010). A strength of this study is the use of our method to construct individual participant level gray matter networks, whereas previous approaches only allowed to construct 1 network across a group of individuals. This method enabled us to investigate associations of gray matter network measures and atrophy rates within individuals. Furthermore, gray matter networks were reconstructed from structural MRI, which is routinely acquired in patient care and therefore has high potential to translate to daily practice.

5. Conclusion

In conclusion, we showed that lower gray matter network measures in early amyloid accumulating regions predict the rate and anatomical pattern of future atrophy in cognitively normal individuals with abnormal amyloid markers. These results suggest that gray matter network measures are a sensitive measure to detect future gray matter atrophy and so may be useful as a tool to select individuals for potential prevention opportunities in the earliest stages of AD.

Disclosure statement

E. Dicks has nothing to disclose. W. M. van der Flier's research programs have been funded by ZonMw, the Netherlands Organization of Scientific Research, Seventh European Framework Program, Alzheimer Nederland, Cardiovascular Onderzoek Nederland, Stichting Dioraphte, Gieskes-Strijbis fonds, Boehringer Ingelheim, Piramal Imaging, Roche BV, Janssen Stellar, Biogen MA and Combinostics. All funding is paid to her institution. F. Barkhof is a consultant for Biogen-Idec, Janssen Alzheimer Immunotherapy, Bayer-Schering, Merck-Serono, Roche, Novartis, Genzume, and Sanofi-Aventis; has received sponsoring from European Commission–Horizon (2020), National Institute for Health Research–University College London Hospitals Biomedical Research Center, Scottish Multiple Sclerosis Register, TEVA, Novartis, and Toshiba; is supported by the University College London Hospitals NHS Foundation Trust Biomedical Research Center; and serves on the editorial boards of Radiology, Brain, Neuroradiology, Multiple Sclerosis Journal, and Neurology. P. Scheltens has acquired grant support (for the institution) from BiogenGE Healthcare, Danone Research, Piramal, and Merck. In the past 2 years, he has received consultancy/speaker fees (paid to the institution) from Lilly, GE Healthcare, Novartis, Sanofi, Nutricia, Probiodrug, Biogen, Roche, Avraham, and EIP Pharma, Merck AG. B. M. Tijms received grant support from ZonMw Memorabel (grant number 73305056).

Acknowledgements

ADNI acknowledgments: Data collection and sharing for this project was funded by the Alzheimer's Disease Neuroimaging Initiative (ADNI) (National Institutes of Health Grant U01 AG024904) and DOD ADNI (Department of Defense award number W81XWH-12-2-0012). ADNI is funded by the National Institute on Aging, the National Institute of Biomedical Imaging and Bioengineering and through generous contributions from the following: AbbVie, Alzheimer's Association; Alzheimer's Drug Discovery Foundation; Araclon Biotech; BioClinica, Inc.; Biogen; Bristol-Myers Squibb Company; CereSpir, Inc.; Cogstate; Eisai Inc.; Elan Pharmaceuticals, Inc.; Eli Lilly and Company; EuroImmun; F. Hoffmann-La Roche Ltd and its affiliated company Genentech, Inc.; Fujirebio; GE Healthcare; IXICO Ltd.; Janssen Alzheimer Immunotherapy Research & Development, LLC.; Johnson & Johnson Pharmaceutical Research & Development LLC.; Lumosity; Lundbeck; Merck & Co., Inc.; Meso Scale Diagnostics, LLC.; NeuroRx Research; Neurotrack Technologies; Novartis Pharmaceuticals Corporation; Pfizer Inc.; Piramal Imaging; Servier; Takeda Pharmaceutical Company; and Transition Therapeutics. The Canadian Institutes of Health Research is providing funds to support ADNI clinical sites in Canada. Private sector contributions are facilitated by the Foundation for the National Institutes of Health (www.fnih.org). The grantee organization is the Northern California Institute for Research and Education, and the study is coordinated by the Alzheimer's Therapeutic Research Institute at the University of Southern California. ADNI data are disseminated by the Laboratory for Neuro Imaging at the University of Southern California. This work was supported by the ZonMw Memorabel Grant Program (BMT; grant number 73305056). Research of the Alzheimer Center Amsterdam is part of the neurodegeneration research program of Amsterdam Neuroscience. The Alzheimer Center Amsterdam is supported by Stichting Alzheimer Nederland and Stichting VUmc Fonds. FB is supported by the NIHR biomedical research center at UCLH.

Author contributions: E.D. processed all image data, performed the statistical analyses, interpreted data, and drafted the manuscript. W.M.v.d.F., F.B., and P.S. interpreted data. B.M.T. was responsible for the study design and concept, contributed to the analyses, and interpreted data. All coauthors have read and critically revised the manuscript.

Appendix A. Supplementary data

Supplementary data to this article can be found online at https://doi.org/10.1016/j.neurobiolaging.2020.05.008.

References

Aisen, P.S., Petersen, R.C., Donohue, M., Weiner, M.W., Alzheimer's Disease Neuroimaging, I, 2015. Alzheimer's disease neuroimaging initiative 2 clinical core: progress and plans. Alzheimers Dement. 11, 734–739.

Alexander-Bloch, A., Giedd, J.N., Bullmore, E., 2013a. Imaging structural co-variance between human brain regions. Nat. Rev. Neurosci. 14, 322–336.

Alexander-Bloch, A., Raznahan, A., Bullmore, E., Giedd, J., 2013b. The convergence of maturational change and structural covariance in human cortical networks. J. Neurosci. 33, 2889–2899.

Bateman, R.J., Xiong, C., Benzinger, T.L., Fagan, A.M., Goate, A., Fox, N.C., Marcus, D.S., Cairns, N.J., Xie, X., Blazey, T.M., Holtzman, D.M., Santacruz, A., Buckles, V., Oliver, A., Moulder, K., Aisen, P.S., Ghetti, B., Klunk, W.E., McDade, E., Martins, R.N., Masters, C.L., Mayeux, R., Ringman, J.M., Rossor, M.N., Schofield, P.R., Sperling, R.A., Salloway, S., Morris, J.C., Dominantly Inherited Alzheimer, N., 2012. Clinical and biomarker changes in dominantly inherited Alzheimer's disease. N. Engl. J. Med. 367, 795–804.

Bates, D., Machler, M., Bolker, B.M., Walker, S.C., 2015. Fitting linear mixed-effects models using lme4. J. Stat. Softw. 67, 1–48.

Braak, H., Braak, E., 1991. Neuropathological stageing of Alzheimer-related changes. Acta Neuropathol. 82, 239–259.

Buckley, R.F., Mormino, E.C., Amariglio, R.E., Properzi, M.J., Rabin, J.S., Lim, Y.Y., Papp, K.V., Jacobs, H.I.L., Burnham, S., Hanseeuw, B.J., Dore, V., Dobson, A., Masters, C.L., Waller, M., Rowe, C.C., Maruff, P., Donohue, M.C., Rentz, D.M., Kirn, D., Hedden, T., Chhatwal, J., Schultz, A.P., Johnson, K.A., Villemagne, V.L., Sperling, R.A., Alzheimer's Disease Neuroimaging, I., Australian Imaging, B., Lifestyle study of, a., Harvard Aging Brain, S., 2018. Sex, amyloid, and APOE epsilon4 and risk of cognitive decline in preclinical Alzheimer's disease: findings from three well-characterized cohorts. Alzheimers Dement. 14, 1193–1203.

Buckner, R.L., Snyder, A.Z., Shannon, B.J., LaRossa, G., Sachs, R., Fotenos, A.F., Sheline, Y.I., Klunk, W.E., Mathis, C.A., Morris, J.C., Mintun, M.A., 2005. Molecular, structural, and functional characterization of Alzheimer's disease: evidence for a relationship between default activity, amyloid, and memory. J. Neurosci. 25, 7709–7717.

Cantero, J.L., Atienza, M., Sanchez-Juan, P., Rodriguez-Rodriguez, E., Vazquez-Higuera, J.L., Pozueta, A., Gonzalez-Suarez, A., Vilaplana, E., Pegueroles, J., Montal, V., Blesa, R., Alcolea, D., Lleo, A., Fortea, J., 2018. Cerebral changes and disrupted gray matter cortical networks in asymptomatic older adults at risk for Alzheimer's disease. Neurobiol. Aging 64, 58–67.

Chetelat, G., Villemagne, V.L., Villain, N., Jones, G., Ellis, K.A., Ames, D., Martins, R.N., Masters, C.L., Rowe, C.C., Group, A.R., 2012. Accelerated cortical atrophy in cognitively normal elderly with high beta-amyloid deposition. Neurology 78, 477–484.

Desikan, R.S., McEvoy, L.K., Thompson, W.K., Holland, D., Roddey, J.C., Blennow, K., Aisen, P.S., Brewer, J.B., Hyman, B.T., Dale, A.M., Alzheimer's Disease Neuroimaging, I., 2011. Amyloid-beta associated volume loss occurs only in the presence of phospho-tau. Ann. Neurol. 70, 657–661.

Dickerson, B.C., Bakkour, A., Salat, D.H., Feczko, E., Pacheco, J., Greve, D.N., Grodstein, F., Wright, C.I., Blacker, D., Rosas, H.D., Sperling, R.A., Atri, A., Growdon, J.H., Hyman, B.T., Morris, J.C., Fischl, B., Buckner, R.L., 2009. The cortical signature of Alzheimer's disease: regionally specific cortical thinning relates to symptom severity in very mild to mild AD dementia and is detectable in asymptomatic amyloid-positive individuals. Cereb. Cortex 19, 497–510.

Dicks, E., Tijms, B.M., Ten Kate, M., Gouw, A.A., Benedictus, M.R., Teunissen, C.E., Barkhof, F., Scheltens, P., van der Flier, W.M., 2018. Gray matter network measures are associated with cognitive decline in mild cognitive impairment. Neurobiol. Aging 61, 198–206.

Dicks, E., Vermunt, L., van der Flier, W.M., Visser, P.J., Barkhof, F., Scheltens, P., Tijms, B.M., Alzheimer's Disease Neuroimaging, I, 2019. Modeling grey matter atrophy as a function of time, aging or cognitive decline show different anatomical patterns in Alzheimer's disease. Neuroimage 22, 101786.

Donohue, M.C., Sperling, R.A., Petersen, R., Sun, C.K., Weiner, M.W., Aisen, P.S., Alzheimer's Disease Neuroimaging, I., 2017. Association between elevated brain amyloid and subsequent cognitive decline among cognitively normal persons. JAMA 317, 2305–2316.

Fjell, A.M., McEvoy, L., Holland, D., Dale, A.M., Walhovd, K.B., Alzheimer's Disease Neuroimaging, I, 2014. What is normal in normal aging? Effects of aging, amyloid and Alzheimer's disease on the cerebral cortex and the hippocampus. Prog. Neurobiol. 117, 20–40.

Fjell, A.M., Walhovd, K.B., Fennema-Notestine, C., McEvoy, L.K., Hagler, D.J., Holland, D., Brewer, J.B., Dale, A.M., 2009. One-year brain atrophy evident in healthy aging. J. Neurosci. 29, 15223–15231.

Gong, G., He, Y., Chen, Z.J., Evans, A.C., 2012. Convergence and divergence of thickness correlations with diffusion connections across the human cerebral cortex. Neuroimage 59, 1239–1248.
He, Y., Chen, Z., Evans, A., 2008. Structural insights into aberrant topological patterns of large-scale cortical networks in Alzheimer's disease. J. Neurosci. 28, 4756–4766.
Ho, A.J., Hua, X., Lee, S., Leow, A.D., Yanovsky, I., Gutman, B., Dinov, I.D., Lepore, N., Stein, J.L., Toga, A.W., Jack Jr., C.R., Bernstein, M.A., Reiman, E.M., Harvey, D.J., Kornak, J., Schuff, N., Alexander, G.E., Weiner, M.W., Thompson, P.M., Alzheimer's Disease Neuroimaging, I, 2010. Comparing 3 T and 1.5 T MRI for tracking Alzheimer's disease progression with tensor-based morphometry. Hum. Brain Mapp. 31, 499–514.
Humphries, M.D., Gurney, K., 2008. Network 'small-world-ness': a quantitative method for determining canonical network equivalence. PLoS One 3, e0002051.
Jack Jr., C.R., Bernstein, M.A., Fox, N.C., Thompson, P., Alexander, G., Harvey, D., Borowski, B., Britson, P.J., J, L.W., Ward, C., Dale, A.M., Felmlee, J.P., Gunter, J.L., Hill, D.L., Killiany, R., Schuff, N., Fox-Bosetti, S., Lin, C., Studholme, C., DeCarli, C.S., Krueger, G., Ward, H.A., Metzger, G.J., Scott, K.T., Mallozzi, R., Blezek, D., Levy, J., Debbins, J.P., Fleisher, A.S., Albert, M., Green, R., Bartzokis, G., Glover, G., Mugler, J., Weiner, M.W., 2008. The Alzheimer's disease neuroimaging initiative (ADNI): MRI methods. J. Magn. Reson. Imaging 27, 685–691.
Jack Jr., C.R., Knopman, D.S., Chételat, G., Dickson, D., Fagan, A.M., Frisoni, G.B., Jagust, W., Mormino, E.C., Petersen, R.C., Sperling, R.A., van der Flier, W.M., Villemagne, V.L., Visser, P.J., Vos, S.J., 2016. Suspected non-Alzheimer disease pathophysiology–concept and controversy. Nat. Rev. Neurol. 12, 117–124.
Jansen, W.J., Ossenkoppele, R., Knol, D.L., Tijms, B.M., Scheltens, P., Verhey, F.R., Visser, P.J., , Amyloid Biomarker Study, G, Aalten, P., Aarsland, D., Alcolea, D., Alexander, M., Almdahl, I.S., Arnold, S.E., Baldeiras, I., Barthel, H., van Berckel, B.N., Bibeau, K., Blennow, K., Brooks, D.J., van Buchem, M.A., Camus, V., Cavedo, E., Chen, K., Chetelat, G., Cohen, A.D., Drzezga, A., Engelborghs, S., Fagan, A.M., Fladby, T., Fleisher, A.S., van der Flier, W.M., Ford, L., Forster, S., Fortea, J., Foskett, N., Frederiksen, K.S., Freund-Levi, Y., Frisoni, G.B., Froelich, L., Gabryelewicz, T., Gill, K.D., Gkatzima, O., Gomez-Tortosa, E., Gordon, M.F., Grimmer, T., Hampel, H., Hausner, L., Hellwig, S., Herukka, S.K., Hildebrandt, H., Ishihara, L., Ivanoiu, A., Jagust, W.J., Johannsen, P., Kandimalla, R., Kapaki, E., Klimkowicz-Mrowiec, A., Klunk, W.E., Kohler, S., Koglin, N., Kornhuber, J., Kramberger, M.G., Van Laere, K., Landau, S.M., Lee, D.Y., de Leon, M., Lisetti, V., Lleo, A., Madsen, K., Maier, W., Marcusson, J., Mattsson, N., de Mendonca, A., Meulenbroek, O., Meyer, P.T., Mintun, M.A., Mok, V., Molinuevo, J.L., Mollergard, H.M., Morris, J.C., Mroczko, B., Van der Mussele, S., Na, D.L., Newberg, A., Nordberg, A., Nordlund, A., Novak, G.P., Paraskevas, G.P., Parnetti, L., Perera, G., Peters, O., Popp, J., Prabhakar, S., Rabinovici, G.D., Ramakers, I.H., Rami, L., Resende de Oliveira, C., Rinne, J.O., Rodrigue, K.M., Rodriguez-Rodriguez, E., Roe, C.M., Rot, U., Rowe, C.C., Ruther, E., Sabri, O., Sanchez-Juan, P., Santana, I., Sarazin, M., Schroder, J., Schutte, C., Seo, S.W., Soetewey, F., Soininen, H., Spiru, L., Struyfs, H., Teunissen, C.E., Tsolaki, M., Vandenberghe, R., Verbeek, M.M., Villemagne, V.L., Vos, S.J., van Waalwijk van Doorn, L.J., Waldemar, G., Wallin, A., Wallin, A.K., Wiltfang, J., Wolk, D.A., Zboch, M., Zetterberg, H., 2015. Prevalence of cerebral amyloid pathology in persons without dementia: a meta-analysis. JAMA 313, 1924–1938.
Koffie, R.M., Meyer-Luehmann, M., Hashimoto, T., Adams, K.W., Mielke, M.L., Garcia-Alloza, M., Micheva, K.D., Smith, S.J., Kim, M.L., Lee, V.M., Hyman, B.T., Spires-Jones, T.L., 2009. Oligomeric amyloid beta associates with postsynaptic densities and correlates with excitatory synapse loss near senile plaques. Proc. Natl. Acad. Sci. U. S. A. 106, 4012–4017.
Koran, M.E.I., Wagener, M., Hohman, T.J., Alzheimer's Neuroimaging, I, 2017. Sex differences in the association between AD biomarkers and cognitive decline. Brain Imaging Behav. 11, 205–213.
Kuchibhotla, K.V., Goldman, S.T., Lattarulo, C.R., Wu, H.Y., Hyman, B.T., Bacskai, B.J., 2008. Abeta plaques lead to aberrant regulation of calcium homeostasis in vivo resulting in structural and functional disruption of neuronal networks. Neuron 59, 214–225.
Kurudenkandy, F.R., Zilberter, M., Biverstal, H., Presto, J., Honcharenko, D., Stromberg, R., Johansson, J., Winblad, B., Fisahn, A., 2014. Amyloid- -induced action potential desynchronization and degradation of hippocampal gamma oscillations is prevented by interference with peptide conformation change and aggregation. J. Neurosci. 34, 11416–11425.
Lobo, A., Launer, L.J., Fratiglioni, L., Andersen, K., Di Carlo, A., Breteler, M.M., Copeland, J.R., Dartigues, J.F., Jagger, C., Martinez-Lage, J., Soininen, H., Hofman, A., 2000. Prevalence of dementia and major subtypes in Europe: a collaborative study of population-based cohorts. Neurologic Diseases in the Elderly Research Group. Neurology 54 (11 Suppl 5), S4–S9.
Maslov, S.S., Sneppen, K., 2002. Specificity and stability in topology of protein networks. Science 296, 910–913.
McKhann, G., Drachman, D., Folstein, M., Katzman, R., Price, D., Stadlan, E.M., 1984. Clinical diagnosis of Alzheimer's disease: report of the NINCDS-ADRDA work group under the auspices of department of Health and human services task force on Alzheimer's disease. Neurology 34, 939–944.
Mechelli, A., Friston, K.J., Frackowiak, R.S., Price, C.J., 2005. Structural covariance in the human cortex. J. Neurosci. 25, 8303–8310.
Noble, W.S., 2009. How does multiple testing correction work? Nat. Biotechnol. 27, 1135.
Palmqvist, S., Scholl, M., Strandberg, O., Mattsson, N., Stomrud, E., Zetterberg, H., Blennow, K., Landau, S., Jagust, W., Hansson, O., 2017. Earliest accumulation of beta-amyloid occurs within the default-mode network and concurrently affects brain connectivity. Nat. Commun. 8, 1214.
Palop, J.J., Chin, J., Roberson, E.D., Wang, J., Thwin, M.T., Bien-Ly, N., Yoo, J., Ho, K.O., Yu, G.Q., Kreitzer, A., Finkbeiner, S., Noebels, J.L., Mucke, L., 2007. Aberrant excitatory neuronal activity and compensatory remodeling of inhibitory hippocampal circuits in mouse models of Alzheimer's disease. Neuron 55, 697–711.
Parnetti, L., Chipi, E., Salvadori, N., D'Andrea, K., Eusebi, P., 2019. Prevalence and risk of progression of preclinical Alzheimer's disease stages: a systematic review and meta-analysis. Alzheimers Res. Ther. 11, 7.
Pereira, J.B., Mijalkov, M., Kakaei, E., Mecocci, P., Vellas, B., Tsolaki, M., Kloszewska, I., Soininen, H., Spenger, C., Lovestone, S., Simmons, A., Wahlund, L.O., Volpe, G., Westman, E., AddNeuroMed consortium, f.t.A.s.D.N.I., 2016. Disrupted network topology in patients with stable and progressive mild cognitive impairment and Alzheimer's disease. Cereb. Cortex 26, 3476–3493.
Petersen, R.C., Aisen, P.S., Beckett, L.A., Donohue, M.C., Gamst, A.C., Harvey, D.J., Jack Jr., C.R., Jagust, W.J., Shaw, L.M., Toga, A.W., Trojanowski, J.Q., Weiner, M.W., 2010. Alzheimer's disease neuroimaging initiative (ADNI): clinical characterization. Neurology 74, 201–209.
Plassman, B.L., Langa, K.M., Fisher, G.G., Heeringa, S.G., Weir, D.R., Ofstedal, M.B., Burke, J.R., Hurd, M.D., Potter, G.G., Rodgers, W.L., Steffens, D.C., Willis, R.J., Wallace, R.B., 2007. Prevalence of dementia in the United States: the aging, demographics, and memory study. Neuroepidemiology 29, 125–132.
Reuter, M., Schmansky, N.J., Rosas, H.D., Fischl, B., 2012. Within-subject template estimation for unbiased longitudinal image analysis. Neuroimage 61, 1402–1418.
Rubinov, M., Sporns, O., 2010. Complex network measures of brain connectivity: uses and interpretations. Neuroimage 52, 1059–1069.
Salehi, A., Delcroix, J.D., Belichenko, P.V., Zhan, K., Wu, C., Valletta, J.S., Takimoto-Kimura, R., Kleschevnikov, A.M., Sambamurti, K., Chung, P.P., Xia, W., Villar, A., Campbell, W.A., Kulnane, L.S., Nixon, R.A., Lamb, B.T., Epstein, C.J., Stokin, G.B., Goldstein, L.S., Mobley, W.C., 2006. Increased App expression in a mouse model of Down's syndrome disrupts NGF transport and causes cholinergic neuron degeneration. Neuron 51, 29–42.
Seeley, W.W., Crawford, R.K., Zhou, J., Miller, B.L., Greicius, M.D., 2009. Neurodegenerative diseases target large-scale human brain networks. Neuron 62, 42–52.
Sekhon, J.S., 2008. Multivariate and propensity score matching software with automated balance optimization: the matching package for R. J. Stat. Softw.
Shankar, G.M., Li, S., Mehta, T.H., Garcia-Munoz, A., Shepardson, N.E., Smith, I., Brett, F.M., Farrell, M.A., Rowan, M.J., Lemere, C.A., Regan, C.M., Walsh, D.M., Sabatini, B.L., Selkoe, D.J., 2008. Amyloid-beta protein dimers isolated directly from Alzheimer's brains impair synaptic plasticity and memory. Nat. Med. 14, 837–842.
Shaw, L.M., Vanderstichele, H., Knapik-Czajka, M., Clark, C.M., Aisen, P.S., Petersen, R.C., Blennow, K., Soares, H., Simon, A., Lewczuk, P., Dean, R., Siemers, E., Potter, W., Lee, V.M., Trojanowski, J.Q., Alzheimer's Disease Neuroimaging, I., 2009. Cerebrospinal fluid biomarker signature in Alzheimer's disease neuroimaging initiative subjects. Ann. Neurol. 65, 403–413.
Sperling, R.A., Aisen, P.S., Beckett, L.A., Bennett, D.A., Craft, S., Fagan, A.M., Iwatsubo, T., Jack Jr., C.R., Kaye, J., Montine, T.J., Park, D.C., Reiman, E.M., Rowe, C.C., Siemers, E., Stern, Y., Yaffe, K., Carrillo, M.C., Thies, B., Morrison-Bogorad, M., Wagster, M.V., Phelps, C.H., 2011. Toward defining the preclinical stages of Alzheimer's disease: recommendations from the National Institute on Aging-Alzheimer's Association workgroups on diagnostic guidelines for Alzheimer's disease. Alzheimers Dement. 7, 280–292.
Sperling, R.A., LaViolette, P.S., O'Keefe, K., O'Brien, J., Rentz, D.M., Pihlajamaki, M., Marshall, G., Hyman, B.T., Selkoe, D.J., Hedden, T., Buckner, R.L., Becker, J.A., Johnson, K.A., 2009. Amyloid deposition is associated with impaired default network function in older persons without dementia. Neuron 63, 178–188.
ten Kate, M., Visser, P.J., Bakardjian, H., Barkhof, F., Sikkes, S.A.M., van der Flier, W.M., Scheltens, P., Hampel, H., Habert, M.O., Dubois, B., Tijms, B.M., 2018. Gray matter network disruptions and regional amyloid beta in cognitively normal adults. Front Aging Neurosci. 10, 67.
Tijms, B.M., Kate, M.T., Wink, A.M., Visser, P.J., Ecay, M., Clerigue, M., Estanga, A., Garcia Sebastian, M., Izagirre, A., Villanua, J., Martinez Lage, P., van der Flier, W.M., Scheltens, P., Sanz Arigita, E., Barkhof, F., 2016. Gray matter network disruptions and amyloid beta in cognitively normal adults. Neurobiol. Aging 37, 154–160.
Tijms, B.M., Möller, C., Vrenken, H., Wink, A.M., de Haan, W., van der Flier, W.M., Stam, C.J., Scheltens, P., Barkhof, F., 2013a. Single-subject grey matter graphs in Alzheimer's disease. PloS One 8, e58921.
Tijms, B.M., Series, P., Willshaw, D.J., Lawrie, S.M., 2012. Similarity-based extraction of individual networks from gray matter MRI scans. Cereb. Cortex 22, 1530–1541.
Tijms, B.M., Ten Kate, M., Gouw, A.A., Borta, A., Verfaillie, S., Teunissen, C.E., Scheltens, P., Barkhof, F., van der Flier, W.M., 2018. Gray matter networks and clinical progression in subjects with predementia Alzheimer's disease. Neurobiol. Aging 61, 75–81.
Tijms, B.M., Wink, A.M., de Haan, W., van der Flier, W.M., Stam, C.J., Scheltens, P., Barkhof, F., 2013b. Alzheimer's disease: connecting findings from graph theoretical studies of brain networks. Neurobiol. Aging 34, 2023–2036.
Tijms, B.M., Yeung, H.M., Sikkes, S.A., Moller, C., Smits, L.L., Stam, C.J., Scheltens, P., van der Flier, W.M., Barkhof, F., 2014. Single-subject gray matter graph properties and their relationship with cognitive impairment in early- and late-onset Alzheimer's disease. Brain Connect. 4, 337–346.

Tzourio-Mazoyer, N., Landeau, B., Papathanassiou, D., Crivello, F., Etard, O., Delcroix, N., Mazoyer, B., Joliot, M., 2002. Automated anatomical labeling of activations in SPM using a macroscopic anatomical parcellation of the MNI MRI single-subject brain. Neuroimage 15, 273–289.

van Rossum, I.A., Vos, S.J., Burns, L., Knol, D.L., Scheltens, P., Soininen, H., Wahlund, L.O., Hampel, H., Tsolaki, M., Minthon, L., L'Italien, G., van der Flier, W.M., Teunissen, C.E., Blennow, K., Barkhof, F., Rueckert, D., Wolz, R., Verhey, F., Visser, P.J., 2012. Injury markers predict time to dementia in subjects with MCI and amyloid pathology. Neurology 79, 1809–1816.

Verfaillie, S.C.J., Slot, R.E.R., Dicks, E., Prins, N.D., Overbeek, J.M., Teunissen, C.E., Scheltens, P., Barkhof, F., van der Flier, W.M., Tijms, B.M., 2018. A more randomly organized grey matter network is associated with deteriorating language and global cognition in individuals with subjective cognitive decline. Hum. Brain Mapp. 39, 3143–3151.

Villain, N., Chetelat, G., Grassiot, B., Bourgeat, P., Jones, G., Ellis, K.A., Ames, D., Martins, R.N., Eustache, F., Salvado, O., Masters, C.L., Rowe, C.C., Villemagne, V.L., Group, A.R., 2012. Regional dynamics of amyloid-beta deposition in healthy elderly, mild cognitive impairment and Alzheimer's disease: a voxelwise PiB-PET longitudinal study. Brain 135 (Pt 7), 2126–2139.

Villeneuve, S., Rabinovici, G.D., Cohn-Sheehy, B.I., Madison, C., Ayakta, N., Ghosh, P.M., La Joie, R., Arthur-Bentil, S.K., Vogel, J.W., Marks, S.M., Lehmann, M., Rosen, H.J., Reed, B., Olichney, J., Boxer, A.L., Miller, B.L., Borys, E., Jin, L.W., Huang, E.J., Grinberg, L.T., DeCarli, C., Seeley, W.W., Jagust, W., 2015. Existing Pittsburgh Compound-B positron emission tomography thresholds are too high: statistical and pathological evaluation. Brain 138 (Pt 7), 2020–2033.

Voevodskaya, O., Pereira, J.B., Volpe, G., Lindberg, O., Stomrud, E., van Westen, D., Westman, E., Hansson, O., 2018. Altered structural network organization in cognitively normal individuals with amyloid pathology. Neurobiol. Aging 64, 15–24.

Vos, S.J., Xiong, C., Visser, P.J., Jasielec, M.S., Hassenstab, J., Grant, E.A., Cairns, N.J., Morris, J.C., Holtzman, D.M., Fagan, A.M., 2013. Preclinical Alzheimer's disease and its outcome: a longitudinal cohort study. Lancet Neurol. 12, 957–965.

Walsh, D.M., Klyubin, I., Fadeeva, J.V., Cullen, W.K., Anwyl, R., Wolfe, M.S., Rowan, M.J., Selkoe, D.J., 2002. Naturally secreted oligomers of amyloid beta protein potently inhibit hippocampal long-term potentiation in vivo. Nature 416, 535–539.

Wang, L., Benzinger, T.L., Hassenstab, J., Blazey, T., Owen, C., Liu, J., Fagan, A.M., Morris, J.C., Ances, B.M., 2015. Spatially distinct atrophy is linked to beta-amyloid and tau in preclinical Alzheimer disease. Neurology 84, 1254–1260.

Whitwell, J.L., Przybelski, S.A., Weigand, S.D., Knopman, D.S., Boeve, B.F., Petersen, R.C., Jack Jr., C.R., 2007. 3D maps from multiple MRI illustrate changing atrophy patterns as subjects progress from mild cognitive impairment to Alzheimer's disease. Brain 130 (Pt 7), 1777–1786.

Yao, Z., Zhang, Y., Lin, L., Zhou, Y., Xu, C., Jiang, T., 2010. Abnormal cortical networks in mild cognitive impairment and Alzheimer's disease. PLoS Comput. Biol. 6, e1001006.